Polymer 51 (2010) 514–521

Contents lists available at ScienceDirect

Polymer

journal homepage: www.elsevier.com/locate/polymer

Experimental measurement and numerical simulation of viscosity reduction effects in HMMPE containing a small amount of exfoliated organoclay-modified TLCP composite

You Hong Tang [a,*,1], Ping Gao [a,*], Lin Ye [b], Chengbi Zhao [c]

[a] Department of Chemical and Biomolecular Engineering, The Hong Kong University of Science and Technology, Clear Water Bay, Kowloon, Hong Kong, China
[b] Centre for Advanced Materials Technology, School of Aerospace, Mechanical and Mechatronic Engineering, The University of Sydney, Sydney, NSW 2006, Australia
[c] Department of Naval Architecture and Ocean Engineering, South China University of Technology, Guangzhou 510641, China

ARTICLE INFO

Article history:
Received 16 September 2009
Received in revised form
30 October 2009
Accepted 23 November 2009
Available online 3 December 2009

Keywords:
Organoclay-modified
thermotropic LCP
Viscosity reduction
Polyethylene

ABSTRACT

A small amount (1 wt%) of organoclay-modified thermotropic liquid crystalline polymer (TLCP) acting as a viscosity reduction agent in high molecular mass polyethylene (HMMPE) was characterized and compared with purified TLCP (1 wt%) in HMMPE at 190 °C and 230 °C, respectively, where the TLCP displayed nematic and nematic-isotropic biphase structures. In the TLCP/PE blend at 190 °C and 230 °C, dramatic reductions in viscosity were observed with significant improvement in extrudate surface smoothness and an enlarged processing window. For the organoclay-modified TLCP in PE, the viscosity reduction ability of TLCP was further enhanced with viscosity dropped by up to >98.5% and >97.4% at 190 °C and 230 °C and processing window enlarged to >700 s^{-1} and >900 s^{-1} respectively in comparison to that of PE. Moreover, yielding stress, initial transition shear rate and transition region decreased to lower magnitudes than those of the TLCP/PE blend. A phenomenological model was applied to elucidate the mechanism of organoclay, TLCP and PE conformation before and after yielding in the confined capillary environment. A binary flow pattern model was applied to successfully predict the rheological behavior of the blends at 190 °C.

1. Introduction

Blends containing small amounts of a thermotropic liquid crystalline polymer (TLCP) in a matrix of thermoplastic have attracted technical interest in recent years for two main reasons. Firstly, by the use of TLCP to enhance the mechanical properties of the matrix polymer through in situ formation of fibrous TLCP dispersion during processing, it may be possible to develop 'self-reinforced' composites that exploit the outstanding tensile properties of fibers made from LCPs. Secondly, it is known that TLCP can act as a flow modifier, resulting in a substantial reduction in pressure drop during melt extrusion. Previous studies by Chan et al. [1] have shown that a small amount of TLCP (1.0 wt%) added to high molecular weight polyethylene (HMMPE, Marlex HXM TR570) caused drastic bulk viscosity reduction (>95.0%) to occur at 190 °C, when TLCP was in its nematic phase. A significant improvement in extrudate surface smoothness has also been observed, coupled with an increase in the processing window from 34 s^{-1} to up to 1000 s^{-1}. Whitehouse et al. [2] blended 0.2%, 0.5% and 2.0% TLCP with high density polyethylene (HDPE), and the blends were then rheologically characterized at 185 °C when the TLCP was in the nematic regime; substantial viscosity reductions of between 85% and 90% compared with pure HDPE were observed.

It is worth noting that even in early studies of polymer blends containing TLCP, researchers had already attempted to introduce inorganic reinforcements into such blend systems [3]. The addition of inorganic fillers not only enhanced the mechanical properties of the blends but also reduced the anisotropy of the resulting materials [4]. Rheological characterization revealed that TLCP could reduce the melt viscosity of glass-filled thermoplastics [5]. Much work has been published on TLCP systems containing different inorganic solid reinforcements, such as glass fibers [6], carbon black [7], whiskers [8] and silica [9]. Most of the studies have used high inorganic solid reinforcement content and have focused on the balance between the mechanical properties and processability of such blends. In our previous studies [10,11], a dramatic reduction in

* Corresponding authors. Department of Chemical and Biomolecular Engineering, The Hong Kong University of Science and Technology, Clear Water Bay, Kowloon, Hong Kong, China. Tel./fax: +852 23587126.
E-mail addresses: tang@aeromech.usyd.edu.au (Y. H. Tang), kepgao@ust.hk (P. Gao).
[1] Current address: Centre for Advanced Materials Technology, School of Aerospace, Mechanical and Mechatronic Engineering, The University of Sydney, Sydney, NSW 2006, Australia. Tel.: +61 2 9315 2305; fax: +61 2 9351 3760.

0032-3861/$ – see front matter © 2009 Elsevier Ltd. All rights reserved.
doi:10.1016/j.polymer.2009.11.051

bulk viscosity (>95.0%) was also observed when 3 wt% TLCP was blended with a 1 wt% organoclay reinforced HMMPE (Marlex HXM TR571) nanocomposite. Moreover, the processing window increased from 50.2 s^{-1} to more than 400.0 s^{-1}.

Fully exfoliated organoclays with uniform sizes of 15–25 nm in the TLCP matrix [12] were well dispersed, which significantly modified the rheological behavior of TLCP at the nematic temperature of TLCP. The rigidity of the TLCP molecules was enhanced by the organoclay, and the orientation of the TLCP molecules was maintained in the shear direction by the presence of organoclay, even after relaxation for a long period (more than 3600 s). Based on the findings of previous studies, in this study we characterize the rheological behavior of purified TLCP and organoclay-modified TLCP (TC3 white) with 1 wt% in HMMPE matrix by a capillary rheometer at 190 °C and 230 °C, where the TLCP has nematic and nematic-isotropic biphase structures. Schematic drawings of the conformation of organoclay, TLCP molecules and polyethylene molecules before and after yielding are shown. A binary flow pattern model with simulated results is presented and the predicted results show good consistency with experimental data.

2. Experimental

2.1. Materials and sample preparation

The HMMPE, Marlex HXM TR571, with a melt flow index (MFI) of 2.5 g/10 min (ASTM D1238, 190 °C/21.6 kg) was kindly supplied by Phillips Petroleum International Inc., USA. The TLCP, a copolymer containing 30% *p*-hydroxybenzoic acid, 35% hydroquinone and 35% sebacic acid (HBA/HQ/SA), used here was synthesized and kindly supplied by B. P. Chemicals Ltd, UK. The as-received TLCP is a light brown powder that has been characterized previously [13]. The organoclay, Closite 20A modified by dimethyl dihydrogenated tallow ammonium ions, was kindly supplied by Southern Clay Products Inc., USA.

A detailed description of the preparation of TC3 white and the purification of as-received TLCP (i.e. purified TLCP) was provided in other studies [12]. For HMMPE blends, the dried 1 wt% TC3 white (or purified TLCP) in powder form and HMMPE in pellet form were mechanically pre-mixed at room temperature until macroscopically homogeneous. The mixture was then extruded using a Dr. Collin twin screw extruder (Dr. Collin GMBH, Germany) at 190 °C with two-time extrusion at different speeds (75 rad/s and 300 rad/s respectively). The extrudate was palletized and kept dry inside an oven overnight to remove moisture generated during the process.

2.2. Characterization

Controlled strain rheological measurements were carried out using an Advanced Rheometric Expansion System (ARES) (TA Instrument, USA). For all tests reported here, 25 mm parallel plate fixtures were used. All measurements were performed at 190 °C with a 2000 g-cm transducer within the resolution limit of 0.2 g-cm and a 200 g-cm transducer within the resolution limit of 0.02 g-cm. Before testing, equipment was preheated and equilibrated at the test temperature for at least 30 min [12].

The rheological behaviors of the blends were also characterized by a capillary rheometer (CR) (Göttfert Rheograph, 2003A, Germany) at 190 °C and 230 °C. Here, the controlled piston speed mode was used with the round hole capillary dies (nominal L/D ratio equal to 30/1 and die entrance angle 180°). The real die diameters used here were recalibrated before use (Calibrated dies diameters $D = 0.924$ mm and 0.542 mm for the nominal $D = 1.0$ and 0.7 mm dies).

The morphology of the extrudates generated during the capillary rheometric experiment was examined by high resolution scanning electron microscopy (JEOL 6700F, Japan) with the acceleration voltage 5 kV. All samples were sputter-coated with a ~200 Å layer of gold to minimize charging. The samples were quenched by compressed air from a hose placed near the die exit, providing a cooling ring. This 'froze' the structure of the TLCP droplets or fibrils before they could relax completely. Micrographs of the surfaces of these samples were taken after etching with a 10 wt% aqueous sodium hydroxide solution at 75 °C for 30 min.

The hybrid embedded in epoxy was ultramicrotomed with glass knives on an ultracut microtome (Leica ultracut-R ultramicrotomed, Germany) at room temperature to produce sections with a nominal thickness of 100 nm. The sections were transferred to Cu grids. To enhance the phase contrast, the sections were stained with a ruthenium tetraoxide vapor for 2 h. Transmission electron microscopy (TEM) images were obtained with a transmission electron microscope at 200 kV (JEOL 2010, Japan). The 'frozen' extrudate for SEM was used for ultramicrotome. All images were obtained from sample sections microtomed along the flow direction.

The mesophase structures of the liquid-crystalline phase of the TLCP and its organoclay composites were investigated by polarized optical microscopy (POM) using an Olympus microscope BX 50 with a Cambridge shear system CSS450 (Linkam Scientific Instruments, UK) connected to hot stage. The most outstanding feature of this setup was that it permitted investigation of texture changes at different temperatures and under varying shear rates. Mesophase structure images were obtained at different temperatures after preshearing the samples at a low shear rate, i.e. 0.5 s^{-1} for more than 3600 s at 185 °C, to remove any shear history and anchored defects.

3. Results and discussion

3.1. Shear deformation

The linear viscoelasticity and large amplitude stress relaxation tests were performed by an ARES at 190 °C. Complex viscosities in frequency sweep and stress relaxation modulus with strain 300.0% are exhibited in Fig. 1(a) and (b) separately. In Fig. 1(a), little difference is shown between the curves, indicating that the purified TLCP and TC3 white had little influence on the HMMPE matrix in the linear viscoelastic region. Large amplitude stress relaxation tests were performed in the nonlinear region. The curves in Fig. 1(b) show no difference over the entire relaxation periods. All the information demonstrates that the purified TLCP and TC3 white had little effect on the shear deformation of the HMMPE at the above particular conditions.

3.2. Elongation deformation

The effects of purified TLCP and TC3 white on the HMMPE matrix were also characterized using a pressure-driven rheometer. Here, the controlled piston speed mode with the round hole capillary dies at 190 °C and 230 °C was used. Capillary flows are usually considered as simple shear flows. The shear stress is highest near the capillary die wall, where the polymer chains are most likely to be stretched to an extended configuration. This is valid only if the melt shows negligible entrance effects. Entrance effects are caused by the elongational flow due to the converging melt flowing from the reservoir into the capillary die with large contraction ratios. The polymer melt along the centerline will experience the highest stretching rate. It has been observed that such effects are extremely important when anisotropic melts such as TLCPs are studied.

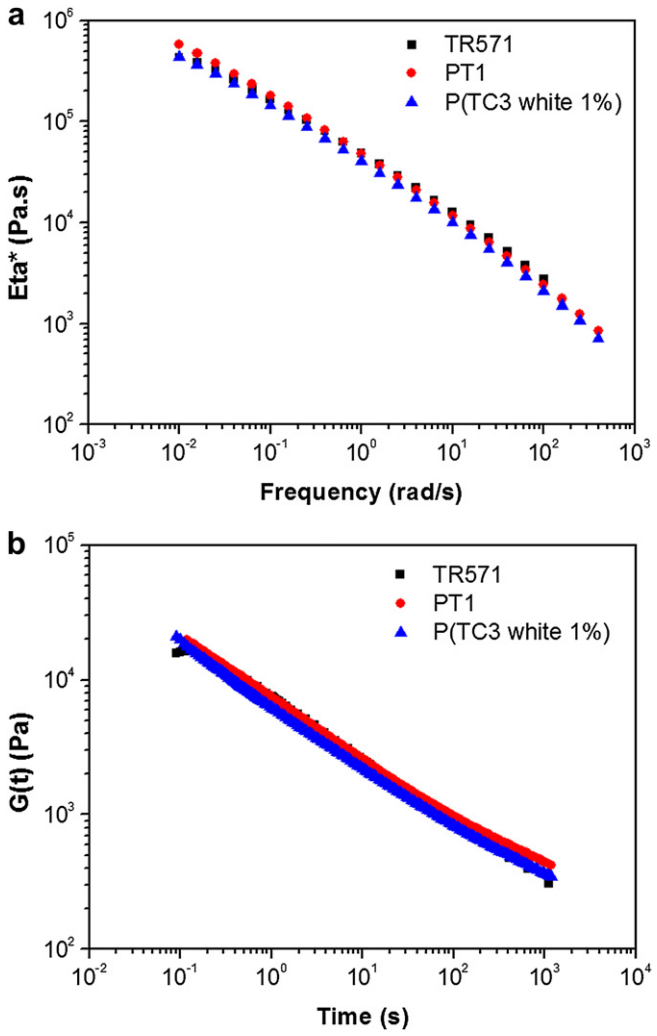

Fig. 1. (a) Dynamic frequency sweep and (b) stress relaxation in nonlinear region with strain = 300.0% of HMMPE [TR571], HMMPE/TLCP 1 wt% [PT1] and HMMPE/(TC3 white 1 wt%) [P(TC3 white 1%)] at 190 °C.

3.2.1. Rheological behavior at 190 °C

Apparent shear viscosities as a function of shear stress at wall for HMMPE [TR571], HMMPE/(purified TLCP 1 wt%) [PT1] and HMMPE/(TC3 white 1 wt%) [P(TC3 white 1%)] with the same L/D ratio (30) and different diameters (0.7 mm and 1.0 m) at 190 °C are shown in Fig. 2. At this temperature, TLCP shows the nematic structures [13]. Significant viscosity reductions are initially observed in different die diameter tests. Based on an equivalent wall stress of 10^5 Pa, the viscosity reductions at 190 °C with $L = 21$ mm and die radius equal to 0.271 mm for the different blends are: for PT1, a similar viscosity to that of HMMPE, because no yielding occurred; for P(TC3 white 1%), 98.5% viscosity reduction compared to HMMPE (corresponding apparent shear rate 317.6 s^{-1}). For the maximum processing rate, HMMPE is ~39 s^{-1}, PT1 is ~318 s^{-1}, whereas P(TC3 white 1%) is up to ~700 s^{-1}. P(TC3 white 1%) can achieve a shear rate almost 20 times higher than that of HMMPE and twice as high as that of PT1.

A yielding-like behavior is shown by all blends when the wall stress is almost constant over a region of rapidly decreasing viscosity. However, yielding stresses and the corresponding beginning and ending apparent shear rates are different for each blend. Table 1 details the yielding behaviors of the blends. From the table, it is clear that with the organoclay-modified, much lower values of yielding stress were needed. Moreover, the apparent

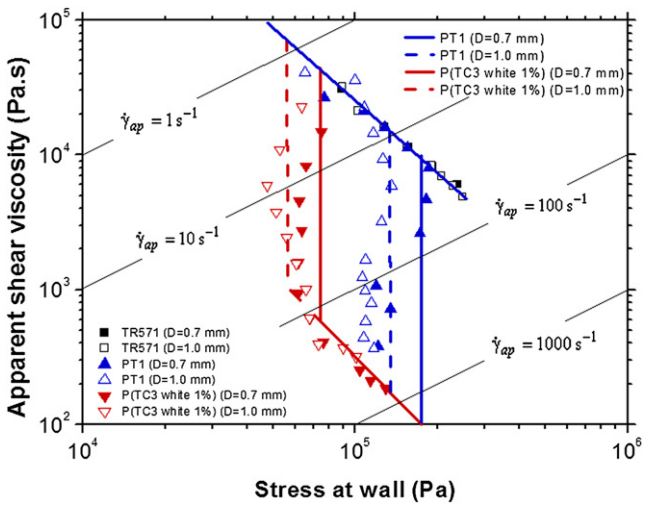

Fig. 2. Apparent shear viscosities as a function of shear stress at wall for HMMPE [TR571], HMMPE/TLCP 1 wt% [PT1] and HMMPE/(TC3 white 1 wt%) [P(TC3 white 1%)] with the same L/D ratio (30) and different diameters (0.7 mm and 1.0 m) at 190 °C with capillary rheometer. (The points were measured data and the lines were simulated data).

shear rate of all blends at the beginning of transition is much lower than that of PT1. This explains why it is difficult to obtain the first power-law region in capillary rheometer tests for P(TC3 white 1%) in simulation, as we describe later in this study. Due to the low yield stress and the initial transition shear rate, the blend can easily move through the transition zone and reach the zone with lower viscosity. The low energy input needed to process the blend holds promising potential for industrial application.

3.2.2. Rheological behavior at 230 °C

The rheological behaviors of three materials at 230 °C are presented with a plot of apparent shear viscosities as a function of shear stress at wall in Fig. 3. At this temperature, TLCP shows nematic/isotropic biphasic structures. Based on an equivalent wall stress of 10^5 Pa, for PT1, the yielding stress is higher than 10^5 Pa, and has similar viscosity to that of HMMPE; for P(TC3 white 1%), a viscosity reduction of >93% was achieved at 230 °C. The maximum processing shear rates are ~66 s^{-1} for HMMPE, ~315 s^{-1} for PT1 and ~904 s^{-1} for P(TC3 white 1%). Table 2 lists the experimental data for yielding stress and transition shear rates for the blends at 230 °C. Similar with the parameters at 190 °C, lower yielding stresses are obtained in PT1 and P(TC3 white 1%). A more obvious phenomenon concerns the transition zone, which is narrow in the range of 8–23 s^{-1} for P(TC3 white 1%) and still cannot obtain transition ending shear rate for PT1. A small force can be used to pass through the narrow transition zone to arrive at the low viscosity region at this temperature for P(TC3 white 1%).

Table 1
Typical parameters with experimental and simulated tests for HMMPE blends at 190 °C (Bold data are predicted results.).

Yielding behaviors	Stress (Pa)		Beginning $\dot{\gamma}_{ap}$ (s^{-1})		Ending $\dot{\gamma}_{ap}$ (s^{-1})	
Dia. (mm)	0.7	1.0	0.7	1.0	0.7	1.0
PT1	**1.63×10^5**	**1.34×10^5**	**41.0**	**24.1**	**855.8**	**476.9**
	1.61×10^5	1.36×10^5	39.8	22.9	–	–
P(TC3 white 1%)	**7.22×10^5**	**5.78×10^5**	**5.6**	**3.3**	**215.7**	**120.1**
	7.08×10^5	5.90×10^5	6.0	3.5	207.4	110.8

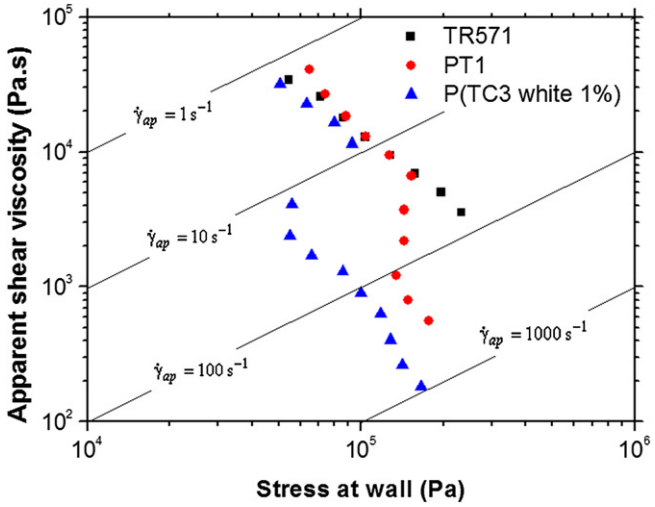

Fig. 3. Apparent shear viscosities as a function of shear stress at wall for HMMPE [TR571], HMMPE/TLCP 1 wt% [PT1] and HMMPE/(TC3 white 1 wt%) [P(TC3 white 1%)] with L/D ratio = 30 and diameter = 1.0 mm at 230 °C with capillary rheometer.

The yielding-like behavior in P(TC3 white 1%) presents an obvious negative gradient. We suggest that the negative gradient is due to TLCP phase transition in the TLCP/organoclay hybrid from isotropic-to-nematic, or maintaining the isotropic phase at that temperature. TLCPs are known and theoretically understood to undergo shear-induced phase transitions when the domain orientation is sufficient high [14,15]. Chan et al. [1] have presented the results of optical microscopy/shearing experiments demonstrating a phase transition from isotropic-to-nematic for this type of TLCP. A pre-transitional order in the isotropic phase of a homologous series of liquid crystals close to the isotropic-to-nematic transition has also been experimentally observed. De Schrijver et al. [16] used a transmission ellipsometric technique to observe this surface-induced isotropic ordering. For the P(TC3 white 1%) blend, since fully exfoliated organoclay structures were formed in the TLCP, no confinement existed to hold an ordered structure and cause phase transition, but there were interactions, such as long-range non-bond forces, which also gave structures more order and retained the orientation even during the relaxation period [12].

3.3. Morphological studies

The SEM diagrams of etched extrudates are shown in Fig. 4 with magnification 20,000. For the HMMPE, as shown in Fig. 4(a), the etched stand gives a rough and highly topological contrast. Moreover, a fine line texture is disclosed after NaOH etching. This indicates that some surface materials or even layers are removed during the etching process. PE is a material that strongly resists attack by NaOH. Therefore, the detached material is thought not to be pure PE. It would be too difficult for NaOH to diffuse into the PE lattice and remove it from the surface. As has already been illustrated by Chan et al. [17] the material removed is an anti-oxidant enrich polyethylene layer, which is caused by migration of anti-oxidant during shear. The surfaces of the blends are smooth at

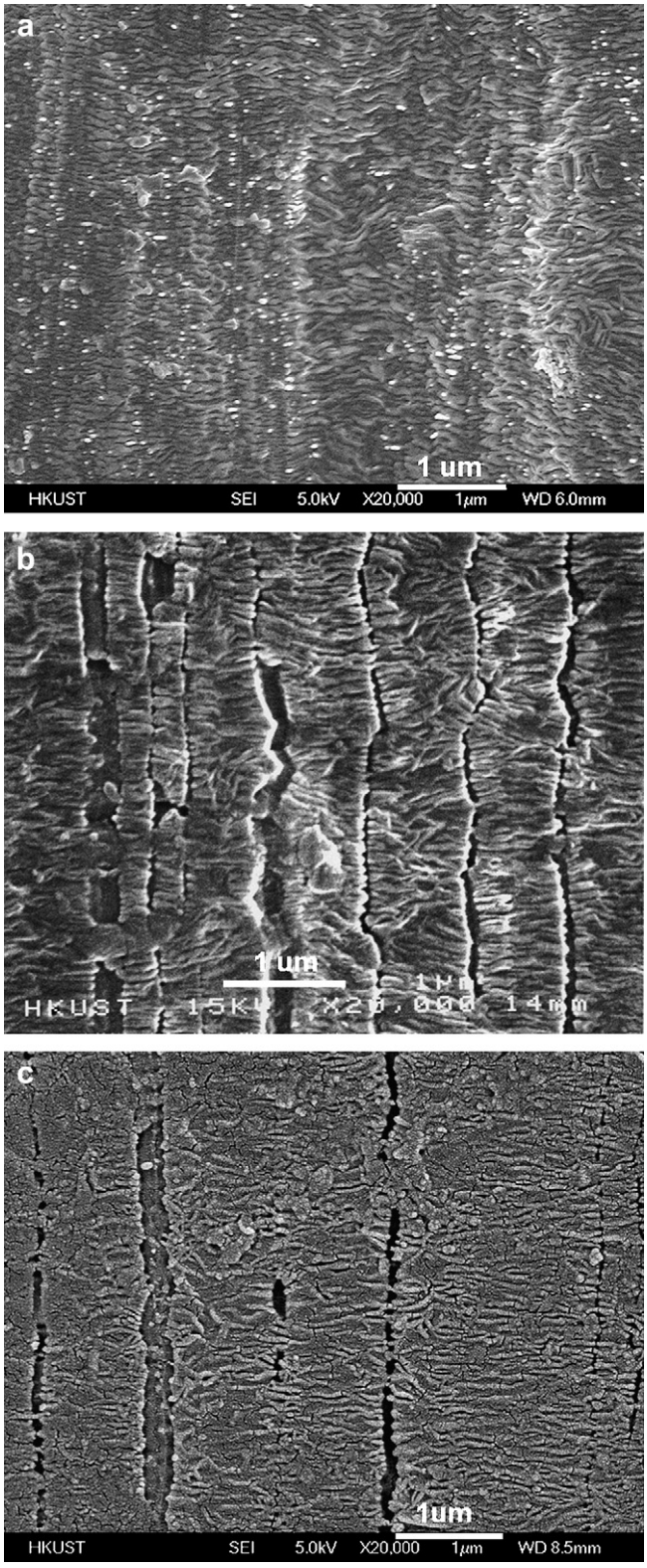

Fig. 4. SEM images of (a) HMMPE [TR571], (b) HMMPE/TLCP 1 wt% [PT1] and (c) HMMPE/(TC3 white 1 wt%) [P(TC3 white 1%)] with magnification 20,000×.

Table 2
Typical parameters with experimental tests for HMMPE blend at 230 °C.

Yielding behaviors	Stress (Pa)	Beginning $\dot{\gamma}_{ap}$ (s^{-1})	Ending $\dot{\gamma}_{ap}$ (s^{-1})
PT1	1.27×10^5	13.6	–
P (TC3 white 1%)	0.56×10^5	8.0	22.9

those apparent shear rates. At higher magnification, some interesting features are revealed. Long and thin cavities are seen, with the long dimension paralleling to the flow direction. These cavities are due to the removal of TLCP filaments. In these well defined

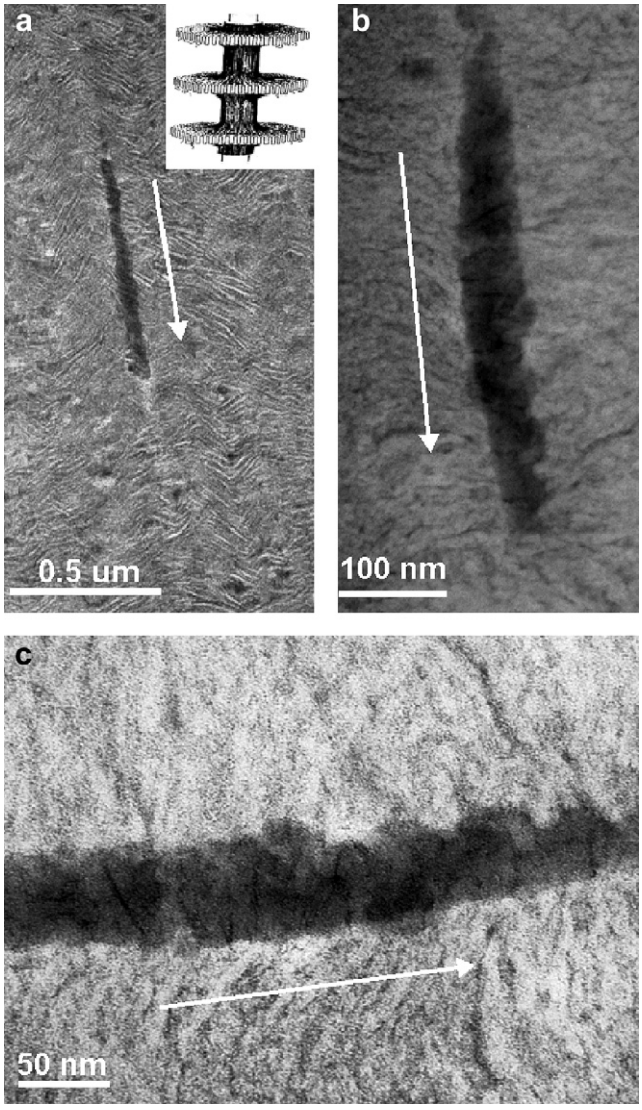

Fig. 5. TEM micrographs of the lateral section of the HMMPE/(TC3 white 1 wt%) [P(TC3 white 1%)] blend extrudate surface prepared parallel to the flow direction at different magnifications.

morphologies: a PT1 strand (Fig. 4(b)) shows only fibrillar structures aligned along the flow direction; also within a P(TC3 white 1%) strand (Fig. 4(c)) only longitudinal fibrillar striations exist. Both images show that in situ fibril formation occurs during elongation in both blends.

TEM images of P(TC3 white 1%) are exhibited in Fig. 5 with different magnifications. Global alignment of PE lamellae can be clearly seen in Fig. 5(a), with typical row-nucleated shish-kebab structures (a schematic drawing in the inset of Fig. 5(a)), a structure which is usually observed when PE crystallization takes place under stress [18,19]. The long fiber crystals formed by the extended high molecular mass fractions act as nucleation sites for the growth of folded PE crystals. Detail micrographs (Fig. 5(b) and (c)) clearly show the strong interfacial compatibilities between the aligned TC3 white filament and the adjacent PE matrix. Also the embedded TC3 white fiber exhibits a regular banded structure, all the bands being perpendicular to the direction of chain alignment. The above observations are similar to those in our earlier studies of PT1 systems [20], indicating that they have a similar viscosity reduction mechanism [21].

3.4. Texture studies

The textures of purified TLCP and TC3 white at 230 °C and 250 °C are presented in Fig. 6 with different magnifications. These samples all underwent the same thermal history with the following steps: (1) sheared at shear rate 0.5 s^{-1} for 3600 s at 185 °C; (2) maintained at this temperature to obtain stable texture; (3) temperature ramped to 230 °C at 5.0 °C/min; (4) obtained texture structure after structure evolution for a specified period. From previous results [12] the purified TLCP and TC3 white displayed a similar texture after steps (1) and (2) at 185 °C. The fully exfoliated organoclay did not affect the liquid crystallinity and mesophase structure at the nematic state at 185 °C. In Fig. 6(a) and (b), an isotropic phase is clearly presented alongside the nematic phase after steady shear at 0.5 s^{-1} for 600 s at 230 °C and relaxation for 600 s for purified TLCP. The nematic phase exists in dispersed and discrete regions containing defect lines, which are highly birefringent and contain domains of anisotropy. The isotropic phase is continuous. There is a distinctly biphasic, nematic/isotropic, texture in purified TLCP at 230 °C. With the elapse of time, a spherical shaped nematic region with a more relaxed state (indicated by the presence of fewer line defects inside the sphere) occurs. Fig. 6(c) presents an image of purified TLCP after shearing at 5.0 s^{-1} for 60 s followed by relaxation for 600 s at 230 °C. The area of continuous isotropic phase has become larger than the nematic phase. With increased of temperature to 250 °C, as Fig. 6(d) shows, the nematic phase gradually diminishes in size and population within the isotropic phase matrix. For TC3 white, as shown in Fig. 6(e) and (f), after steady shearing at 0.5 s^{-1} for 600 s followed by relaxation for 600 s, a dominant nematic texture occurs with few dispersed isotropic regions at 230 °C. The defects which were stable at 185 °C become unstable at 230 °C, due to the effect of the high temperature. As time elapses, the isotropic phase occurs in a minority of discrete regions, and the nematic phase is still dominant. Even after steady shearing at a high shear rate 5.0 s^{-1} for 60 s followed by relaxation for 600 s at 230 °C, the nematic phase still exists as a continuous structure with a few discrete isotropic structures, as shown in Fig. 6(g). The exfoliated organoclays enhance the rigidity of the TLCP molecules and keep them in ordered structures at the high temperature. The competition between the high thermal energy and the internal molecular interactions of the organoclay and TLCP molecules causes the nematic phase to be dominated by biphasic structures for TC3 white at 230 °C. Even at a higher temperature, i.e. 250 °C, after 5.0 s^{-1} shearing for 60 s followed by relaxation for 300 s, the nematic phase is still in continuous mode, as Fig. 6(h) shows.

For the organoclay-modified TLCP, i.e. TC3 white, the combination of the above mentioned nematic dominated structure and shear-induced isotropic–nematic transition had the effect that its rheological behavior at 230 °C was similar to that at 190 °C, with even a higher processing window and a lower transition region.

3.5. Predictions based on a phenomenological model

A binary flow pattern model, previously used for prediction of the effects of a small amount of TLCP in HMMPE (Marlex HXM TR570) [21] was used to simulate the rheological responses of the blends in this study.

3.5.1. Model

To account for the structural effects due to elongational flow along the centerline region in the capillary die, the overall melt flow characteristics are divided into three regions depending on the magnitude of the maximum fluid velocity in the capillary that is usually along the centerline in converging flows. This critical fluid

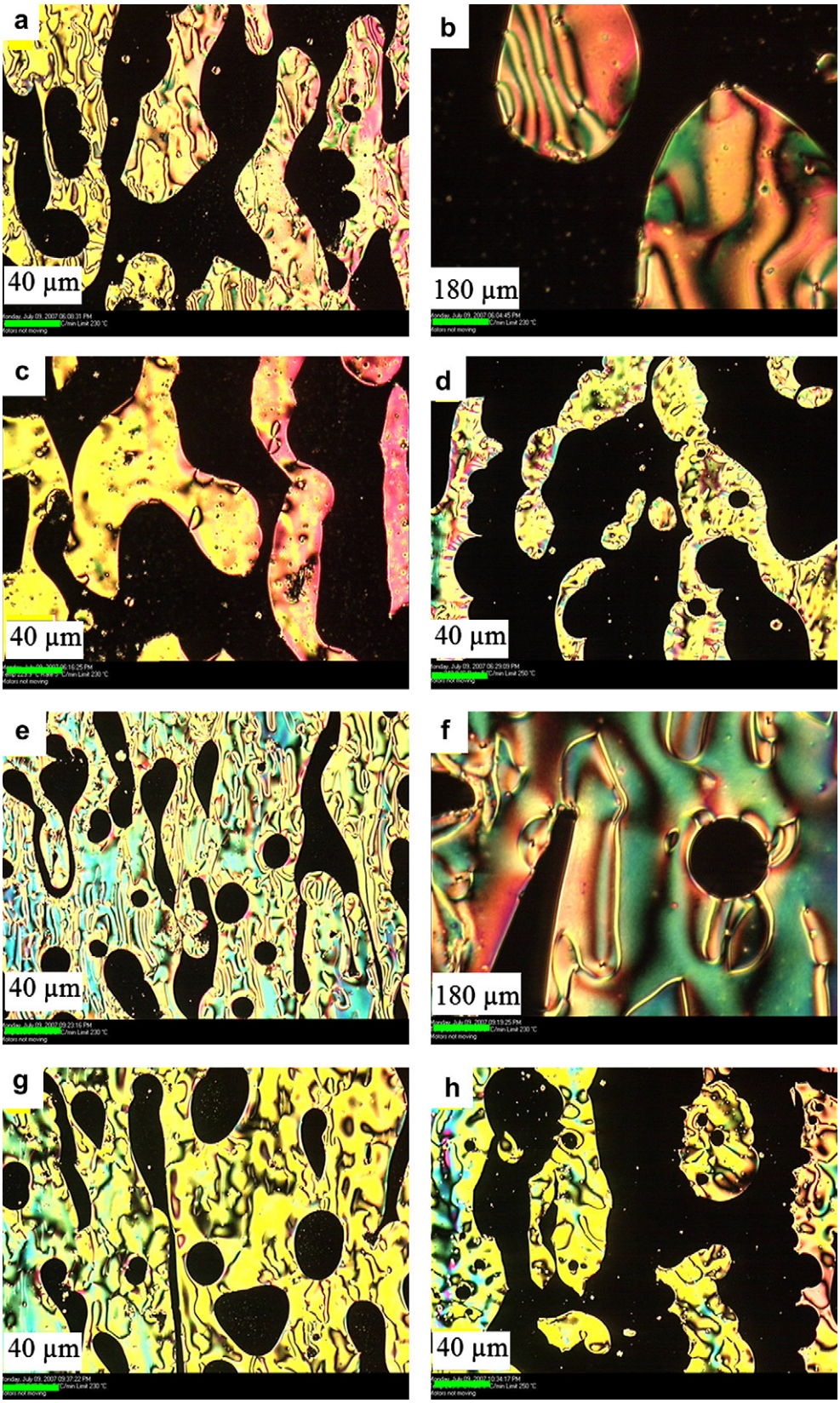

Fig. 6. Polarized optical microscope images of (a) and (b) purified TLCP and (e) and (f) TC3 white relaxed for 600 s at 230 °C after steady shear with 0.5 s^{-1} for 600 s; (c) purified TLCP and (g) TC3 white relaxed for 600 s at 230 °C after steady shear with 5.0 s^{-1} for 60 s; (d) purified TLCP and (h) TC3 white relaxed for 300 s at 250 °C after steady shear with 5.0 s^{-1} for 60 s (all samples have been sheared with shear rate 0.5 s^{-1} for 3600 s and relaxed to steady state at 185 °C).

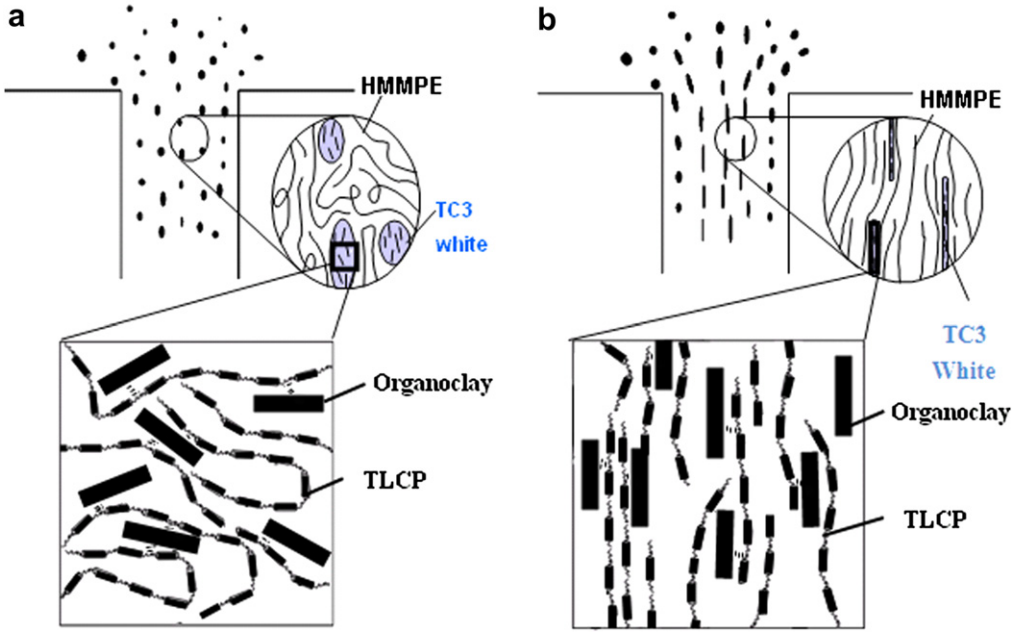

Fig. 7. Schematic drawing of HMMPE chains, TLCP chains and organoclay morphological change in capillary die at 190 °C (a) before and (b) after critical shear rates.

velocity corresponds to the maximum stretching rate of the TLCP (or TC3 white) domains at which irreversible TLCP (or TC3 white) domain elongation into slender filament occurs. The three regimes are:

Region I: The fluid velocity is below the critical velocity for irreversible TLCP (or TC3 white) domain elongation, and the flow of the blends is dominated by the melt flow behavior of the matrix polymer HMMPE melt, independent of TLCP (or TC3 white). A schematic illustration of the melt structure during flow in Region I is shown in Fig. 7(a). PE chains formed random coiled conformation and TLCP (or TC3 white) has ellipse shapes with uniformed dispersion in PE matrix. The inset in Fig. 7(a) shows the organoclay and TLCP chain conformation at this region. Organoclays of uniform size were well and irregularly dispersed in the nematic phase TLCP.

Region II: The maximum fluid velocity within the capillary reaches the critical velocity at the entrance of the capillary and irreversible elongational deformation of the TLCP (or TC3 white) domains into long slender fibrous forms begins to occur. This causes a rapid chain elongation and disengagement in the PE melt adjacent to the TLCP (or TC3 white) domains. Consequently, a region of low viscosity melt is formed in the center core of the capillary die. This center region expands as the flow rate increases until all fluid within the capillary is filled with such melt. The simulated velocity profile developments of fluid flowing through a capillary die to describe the above phenomenon will be presented later in this study. A schematic illustration of the melt structure during flow in Region II is shown in Fig. 7(b). The inset in Fig. 7(b) shows the chain conformations of TLCP molecules with help of organoclay. Shear-induced molecular alignment occurs with TLCP molecules and organoclay oriented along the elongation direction.

Region III: After all low viscosity fluid is formed across the entire capillary die diameter, a homogeneous melt flow corresponding to the low viscosity melt may be assumed again.

3.5.2. Velocity profiles

The velocity profile developments of fluid flowing through capillary dies are shown in Fig. 8. As shear rate increases, the center core region characterized by low viscosity melt flow characteristics expands from the center core towards the die wall. Close to the

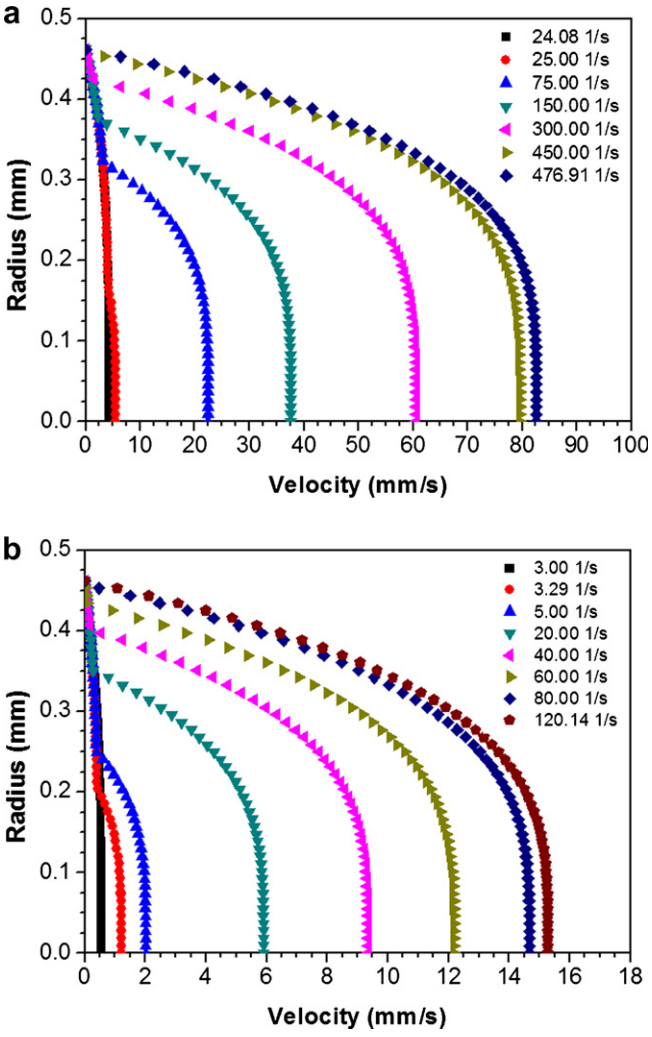

Fig. 8. Velocity profile development in region II of flow at $R = 0.462$ mm for (a) HMMPE/TLCP 1 wt% and (b)HMMPE/TC3 white 1 wt% at 190 °C by simulation.

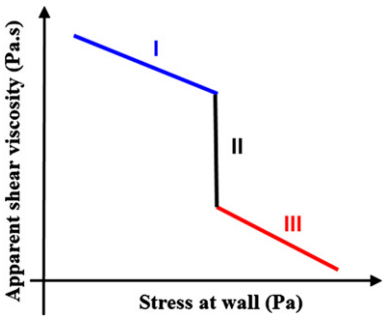

Fig. 9. Schematic drawing of apparent shear viscosity evolution as a function of stress at wall at different stages in capillary die at 190 °C.

wall, the velocity profiles are independent of apparent shear rates. This implies that the shear rates at the wall are independent of flow rates of fluid during the melt structure transition period. Consequently, the wall shear stresses will remain constant throughout this transition period. In the velocity profiles for the different blends, the real die diameters were used instead of the nominal diameters. For nominal diameters 1.0 mm and 0.7 mm, the real calibrated diameters were 0.924 mm and 0.542 mm. Table 1 shows the predicted yielding stress and transition shear rates with the experimental data. The predicted data coincide well with the experimental results. The prediction results also give the end transition shear rates for PT1 at 190 °C with different die diameters, which cannot be obtained experimentally due to the flow oscillation.

3.5.3. Flow curves simulation

The flow curves are divided into three regimes as described above. In Regions (I) and (III), simple power-law constitutive relations are assumed. In Region (I), because of the relatively lower yielding shear rates for these blends, dynamic frequency sweep data performed on ARES were used combined with data from CR for simulation. The flow curves in Region (II) were obtained using the velocity profiles together with the power-law parameters in Regions (I) and (III). Fig. 9 shows the schematic drawing of apparent shear viscosity as a function of shear stress at wall at the different stages in capillary die. Precise flow curves with Matlab program simulation for the blends are plotted in Fig. 2 together with experimental data. Excellent agreement between the model prediction and the experimentally measured flow curves is obtained.

4. Conclusions

The rheological behaviors of purified thermotropic liquid crystalline polymer (purified TLCP) and fully exfoliated organoclay-modified TLCP (TC3 white) in high molecular mass polyethylene (HMMPE) were characterized by capillary rheometer (CR) with nominal dies of $L/D = 30$ and diameters 0.7 mm and 1.0 mm at 190 °C, where purified TLCP and TC3 white showed similar nematic phase structures. At 230 °C, purified TLCP presented as a continuous isotropic phase with a minority of discrete nematic phase, whereas TC3 white displayed a continuous nematic phase with a few isotropic phases. The interactions between organoclays with TLCP molecules at the molecular level enhanced the rigidity of the TLCP molecules, displaying the nematic order structure even at higher temperature. The rheological experiments using CR with a nominal die of $L/D = 30$ and diameter 1.0 mm showed even higher viscosity reduction ability with a wider processing window for TC3 white than for the purified TLCP in the PE matrix. In addition, a much lower yielding stress with a narrower transition window was obtained in the TC3 white/PE blend than in the purified TLCP/PE blend. These findings have promising potential for industrial application to save energy and increase processing efficiency when used in processing such thermoplastics. Mechanism study confirmed that the binary flow model can be applied to describe the rheological behaviors of both blends and shear-induced phase transitions and alignment of in situ formation of fibrils are the primary reasons for viscosity reduction.

Acknowledgements

This project was funded by a grant from the Research Grant Council of Hong Kong, grant number HKUST6256/02.

References

[1] Chan CK, Whitehouse C, Gao P. Polym Eng Sci 1999;39:1353–64.
[2] Whitehouse C, Lu XH, Gao P, Chai CK. Polym Eng Sci 1997;37:1944–58.
[3] Baird DG, Wilkes GL. Polym Eng Sci 1983;23:632–6.
[4] Bafna SS, de Souza JP, Sun T, Baird DG. Polym Eng Sci 1993;33:808–18.
[5] Kulichikhin VG, Parsamyan IL, Lipatov YS, Shumskii VF, Getmanchuk IP, Babich VF, et al. Polym Eng Sci 1997;37:1314–21.
[6] Pisharath S, Wong SC. Polym Compos 2003;24:109–18.
[7] Tchoudakov R, Narkis M, Siegmann A. Polym Eng Sci 2004;44:528–40.
[8] Tjong SC, Meng YZ. Polymer 1999;40:7275–83.
[9] Lee MW, Hu X, Yue CY, Li L, Tam KC. Compos Sci Technol 2003;63:339–46.
[10] Tang YH, Yang HM, Gao P. J Cent South Univ Technol 2007;14:192–6.
[11] Tang YH, Gao P, Ye L, Zhao CB. Polym Eng Sci, submitted for publication.
[12] Tang YH, Gao P, Ye L, Zhao CB. J Polym Sci Part B Polym Phys, submitted for publication.
[13] Gao P, Lu XL, Chai CK. Polym Eng Sci 1996;36:2771–80.
[14] Mather PT, Romo-Uribe A, Han CD, Kim SS. Macromolecules 1997;30:7977–89.
[15] Han CD, Kim SS. Macromolecules 1995;28:2089–92.
[16] de Schrijver P, van Dael W, Thoen J. Liq Cryst 1996;21:745–9.
[17] Chan CK, Whitehouse C, Gao P, Chai CK. Polymer 2001;42:7847–56.
[18] Yu TH, Wilkes GL. J Rheol 1996;40:1079–93.
[19] Zhou H, Wilkes GL. J Mater Sci 1998;33:287–303.
[20] Chan CK, Gao P. Polymer 2005;46:10890–6.
[21] Chan CK, Gao P. Polymer 2005;46:8151–6.